
Articles

2023

Structural, Thermal, Optical, and Mechanical Properties of Composite Films Developed from the Button Mushroom (*Agaricus bisporus*)-Sourced High Molecular Weight Chitosan and Potato Starch

Buliyamini Alimi

Technological University Dublin, Ireland, buliyaminu.alimi@tudublin.ie

Monjural Hoque


Teagasc Food Research Centre, Dublin, Ireland

Shivani Pathania

Teagasc Food Research Centre, Dublin, Ireland

See next page for additional authors

Follow this and additional works at: <https://arrow.tudublin.ie/creaart>

 Part of the [Materials Chemistry Commons](#), and the [Polymer Chemistry Commons](#)

Recommended Citation

Alimi, Buliyamini; Hoque, Monjural; Pathania, Shivani; Wilson, Jude; Duffy, Brendan; and Frias, Jesus Maria, "Structural, Thermal, Optical, and Mechanical Properties of Composite Films Developed from the Button Mushroom (*Agaricus bisporus*)-Sourced High Molecular Weight Chitosan and Potato Starch" (2023). *Articles*. 237.

<https://arrow.tudublin.ie/creaart/237>

This Article is brought to you for free and open access by ARROW@TU Dublin. It has been accepted for inclusion in Articles by an authorized administrator of ARROW@TU Dublin. For more information, please contact arrow.admin@tudublin.ie, aisling.coyne@tudublin.ie, vera.kilshaw@tudublin.ie.



This work is licensed under a [Creative Commons Attribution-Share Alike 4.0 International License](#).

Funder: This work was supported by Marie Slodowska-Curie and Enterprise Ireland through CAREER-FIT PLUS Fellowship (MF 2021 0199) granted to Dr Buliyaminu Adegbemiro Alimi

Authors

Bullyamini Alimi, Monjural Hoque, Shivani Pathania, Jude Wilson, Brendan Duffy, and Jesus Maria Frias



Structural, thermal, optical, and mechanical properties of composite films developed from the button mushroom (*Agaricus bisporus*)-sourced high molecular weight chitosan and potato starch

Buliyaminu Adegbemiro Alimi^{a,*}, Monjurul Hoque^b, Shivani Pathania^b, Jude Wilson^c, Brendan Duffy^d, Jesus Maria Celayeta Frias^a

^a Environmental Sustainability and Health Institute, Technological University Dublin, Ireland

^b Food Industry Development Department, Teagasc Food Research Centre, Ashtown, Dublin, 15, Ireland

^c MBio, Monaghan Mushrooms, Tyholland, Co. Monaghan, Ireland

^d Centre for Research in Engineering and Surface Technology (CREST), FOCAS Institute, Technological University Dublin-City Campus, Kevin Street, Dublin, D08 NF82, Ireland

ARTICLE INFO

Keywords:

Food packaging
Circularity
Biopolymers
Rheological properties
Hydrogen bonding
Light transmittance

ABSTRACT

Films were fabricated using the button mushroom (*Agaricus bisporus*) sourced high molecular weight chitosan with or without potato starch using the casting method. Glycerol was used as the plasticizer. Chitosan content in the film-forming solution (FFS) was varied (0.5, 0.75 and 1.0% w/v of FFS) while potato starch (1.0% of FFS) and glycerol (25% of the total solid content in the solution) contents were not varied. The control sample contained only chitosan (1.0% of the FFS) and glycerol. The effect of increasing the content of chitosan on the rheological properties of FFS and the properties of the films were investigated. The FFS's shear viscosity and shear modulus (elastic and viscous components) increased with increasing chitosan content. Morphological examination revealed that the films exhibited a compact structure devoid of large pores and cracks. Surface roughness captured with an atomic force microscope was reduced (19-6 nm) with increasing content of chitosan in the film. The films exhibited two hydrated crystalline phases at 9 and 20°. Light transmittance and glossiness of the films were enhanced with increasing chitosan content. FTIR analysis indicated the increasing availability of reactive sites with the increasing content of chitosan leading to an enhanced hydrogen bonds network and increased cohesion of the film structure. This may be the reason for improved mechanical properties and reduced water vapour permeability of the films with increasing chitosan content.

1. Introduction

Despite its associated challenges to human health safety, the environment and the economy, petroleum-based polymers remain the leading materials for food packaging applications. However, the recent spike in research efforts for the development of functional packaging materials from natural biopolymers may ultimately present the possibility of eco-friendly alternatives (Liu et al., 2020; Alimi, Workneh, & Zubair, 2022). Besides solving the problems associated with petroleum-based polymers, these natural biopolymers also have the advantages of circularity, renewability and sustainability (Liu et al., 2012; Alimi, Workneh & Femi, 2021). Chitosan, a deacetylated derivative of chitin (the second most ubiquitous natural polymer on earth) has

attracted research attention for its film-forming capability. It has been shown to possess film-forming, functional and biological properties (Lin et al., 2020). Chitosan has the unique advantage of being the only polycationic polymer in nature (Ma, Qiao, Wang, Yao, & Xu, 2019; Madeleine-Perdrillat et al., 2015). The polycationic backbone of chitosan is one of the probable factors responsible for its antimicrobial property (van den Broek, Knoop, Kappen, & Boeriu, 2015). Chitosan materials have also shown an ability to chelate heavy ions and hypocholesterolemic activity (Rajoka, Zhao, Mehwish, Wu, & Mahmood, 2019; Lipatovaa, Losev, Makarovaa, Rodicheva, & Burmistrov, 2020).

The film-forming capability of chitosan has been exploited in the development of edible films and other food packaging materials (Ma et al., 2019). However, the use of chitosan singly in film forming has some

* Corresponding author.

E-mail address: Buliyaminu.Alimi@TuDublin.ie (B.A. Alimi).

<https://doi.org/10.1016/j.lwt.2023.115201>

Received 29 April 2023; Received in revised form 8 July 2023; Accepted 16 August 2023

Available online 17 August 2023

0023-6438/© 2023 The Authors. Published by Elsevier Ltd. This is an open access article under the CC BY license (<http://creativecommons.org/licenses/by/4.0/>).

technological challenges. The highly hygroscopic nature of chitosan is a major setback to its use in film development since the absorbed moisture could weaken the structure and mechanical strength of the developed film (Ma et al., 2019). Films developed from chitosan alone exhibited poor flexibility and extensibility (Prateepchanachai, Thakhiew, Devahastin, & Soponronnarit, 2017). The challenge of extensibility is easily solved with the inclusion of a plasticizer (especially polyols) in the film-forming solution. The inclusion of glycerol, in the range of 20–25% solid content, in chitosan film-forming solution was reported to enhance the flexibility and extensibility of chitosan film (Rodríguez-Núñez, Madera-Santana, Sánchez-Machado, López-Cervantes, & Soto Valdez, 2014).

Blending with other film-forming materials such as natural polymers, polylactic acid (PLA), polyhydroxybutyrate (PHB), poly-ε-caprolactone (PCL) is often employed to improve the mechanical properties of chitosan films (van den Broek et al., 2015). However, high cost and fragility are the main challenges of the use of PLA, PHB and PCL in film development for food applications (Claro et al., 2016). Comparatively, starch has lower cost, abundant availability, superior film-forming ability, and relative stability over other natural polymers such as lipids and proteins (Alimi et al., 2022).

Films have been prepared from chitosan alone or in combination with other polysaccharides for enhanced properties (Liu et al., 2020). Starches from different sources such as wheat (Bonilla, Atarés, Vargas, & Chiralt, 2013), corn and rice (Ren, Yan, Zhou, Tong, & Su, 2017), and potato (Lipatova, Losev, Makarova, Rodicheva, & Burmistrov, 2020) have been blended with chitosan for film development. Improved mechanical properties and water vapour permeability over films obtained from either chitosan or starch alone present an interesting outlook for the prospective application of composite chitosan-starch films in food packaging. Chitosan-based films and coatings have been applied in the quality protection of some fruits and vegetables (Oladzadabbasabadi et al., 2022).

Chitosan is mostly derived from chitin sourced from marine waste (Ghormade, Pathan & Deshpande, 2017). However, fungal-sourced chitosan is attracting research and commercial interest due to some advantages it has over marine-sourced chitosan. It offers a friendly alternative to vegans, does not contain compounds such as tropomyosin, myosin light chain and arginine kinase known to trigger allergic reactions and was reported to offer a greater possibility of control of physicochemical properties (Hassainia, Satha, & Boufi, 2018). Fungal-derived chitosan production can be sustainable since filamentous fungi (such as mushrooms) can be grown under controlled conditions throughout the year. This is unlike marine animals' by-products, whose availability is seasonal (Ospina Álvarez et al., 2014). Also, fungi have low organic matter, and hence, would require a cost-effective mild treatment for chitin/chitosan extraction (Kaya, Kahyaoglu, & Sumnu, 2022).

Mushrooms are macro-fungi whose parts are replete with chitin that is easily converted to chitosan. The global market value of the mushroom business was reported to be in the region of US\$ 63 Billion. There is also a projection that annual sales of mushrooms would increase from 34 to 60 billion US dollars in the next few years (Grimm & Wösten, 2018). Some reports put *Agaricus bisporus* (button mushroom) as the most cultivated edible species, representing 40% of total global production (Martinez-Medina et al., 2021; Marçal et al., 2021; Rathore, Prasad, & Sharma, 2017). With the above advantages and high production volumes, *A. bisporus* can be considered a source of chitosan (Kaya et al., 2022). Chitosan has been successfully extracted from *A. bisporus* (Kannan, Nesakumari, Rajarathinam, & Singh, 2010; Wu, Niu, Jiao, & Chen, 2019). We are unaware of any report on developing composite films from chitosan sourced from *A. bisporus*.

The film forming capabilities of high and low molecular (MW) chitosan from *A. bisporus*, with and without potato starch, were compared in our preliminary studies. Our findings affirmed previous reports that high MW chitosan is the ideal for film development (Liu et al., 2012; Liu et al., 2020). Thus, the objective of this study was to evaluate the

film-forming potential of high MW chitosan from *A. bisporus* with or without potato starch, which has not been tested before.

2. Materials and methods

2.1. Materials

High MW *A. bisporus* chitosan (formula: $(C_6H_{11}NO_4)_n$); viscosity: 1000 mPa s; MW: ≈ 1490.4 kDa) was purchased from Qingdao ChiBio Biotech Co., Ltd, China. Finnegan's Farm, Navan, Co. Meath, Ireland supplied potato starch in kind. Glycerol (1,2,3-Propanetriol, Glycerin) and Acetic acid ($\geq 99.5\%$) were purchased from Merck Life Science Limited (Sigma-Aldrich), Arklow, Ireland. All chemicals are of food grade.

2.2. Film preparation

A method described by Liu, Zhou, Zhang, Yu, and Cao (2014) was modified to prepare the film-forming solution (FFS). Chitosan was dissolved in a 2% v/v acetic acid solution to make 0.5, 0.75 and 1% w/v of FFS. The chitosan solution was stirred for 2 h at 50 °C for complete dissolution. Potato starch (1% w/v of the FFS) and glycerol (25% of the total solid content) were added separately during stirring. An FFS containing chitosan (1.0% of the solution), glycerol (25% of the total solid content) and without potato starch inclusion was prepared to serve as the control sample. The mixture was heated at 90 °C with continuous stirring until a colourless and viscous liquid was formed (≈ 1 h). The film-forming solution was placed on ice water to cool and then degassed under a vacuum. An aliquot of the cooled solution (30 g) was dispensed into an acrylic petri-dish (12 × 12 mm) and dried in a convective oven (50 °C for 24 h). After drying, the films were carefully peeled and stored in a controlled humidity and temperature chamber (Mettler GmbH + Co. KG Büchenbach, Germany) at 25 °C and 55% relative humidity for conditioning and held under the condition until analysis.

2.3. Rheological properties of the film-forming solutions

The rheological properties of the film-forming solutions were determined using Kinexus Rotational Rheometer (NETZSCH, Bavaria, Germany). Viscosity was measured at a shear rate of 1/s for 5 min at 25 °C and data was taken at an interval of 2 s.

The modulus of the film-forming solutions was determined at a single frequency of 1 Hz, shear strain of 1%, test time of 5 min, a temperature of 25 °C and data intervals of 5 s. The heat stabilisation period for both measurements was 2.5 min, and the tests were performed in triplicate.

2.4. Characterisation of the films

2.4.1. Morphological characterisation

2.4.1.1. Surface and cross-sectional structures of the films. The surface morphology of the films was characterised using a high-resolution field emission scanning electron microscope (Hitachi SU-70, Hitachi High-Tech Corporation, Tokyo, Japan). A small fragment of the film samples coated with platinum was mounted on stubs using double-sided tapes and afterwards placed inside the chamber of the microscope operating at a resolution of 1.0 nm at 15 KV. For cross-section microstructure, the films were cryo-fractured with liquid Nitrogen, mounted vertically and platinum-coated prior to observation with the SEM.

2.4.1.2. Surface roughness. A 3-D image and roughness of the surfaces of the films were obtained using an atomic force microscope (AFM) MFP-3D BIO (Asylum Research, Oxford Instruments, Santa Barbara, CA 93117, United States).

2.4.2. X-ray diffraction

The diffraction patterns of the films were observed using Rigaku Miniflex Benchtop X-Ray Diffractometer (Rigaku Corporation, Akishima-shi, Tokyo, Japan). The diffractometer was operated at Bragg angle 2θ in the range $3\text{--}50^\circ$, scan step of 0.035° and, generator settings of 40 KV and 40 mA.

2.4.3. Optical properties

A PerkinElmer Lambda 900 UV/VIS/NIR spectrometer (Beaconsfield, UK) was used to measure the light transmittance of the films. Films were placed inside the spectrometer to allow light to pass through directly. Measurement was taken at 560 nm.

A dual-angle gloss meter (Elcometer, Manchester, England) operating at 20 and 60° was used to measure the glossiness of 50×50 mm film cut.

2.4.4. FTIR

A dual-range Spectrum 400 series spectrometer (PerkinElmer, Beaconsfield, UK) was used to capture the infrared spectra of the films. The spectra were captured at a range of 4000 to 380 cm^{-1} at a spectra resolution of 4 cm^{-1} in the infrared region.

2.4.5. Thermal properties

A thermogravimetric analyser (TGA/DSC 3+ STAR^e system, METTLER TOLEDO, USA) operating under a nitrogen atmosphere at a flow rate of 50 mL/min was used to assess the thermal stability of the films. A known weight of the film sample was placed in an aluminium pan and sealed. An empty pan of the same type was used as a reference. The samples were evaluated using the temperature protocol, which involved heating the samples at a rate of $10\text{ }^\circ\text{C/min}$ from $30\text{ }^\circ\text{C}$ to $650\text{ }^\circ\text{C}$.

2.4.6. Thickness

A handheld digital micrometre with a precision of 0.001 mm was used to determine the thickness of the films taken at 10 different points in each film. The average of the readings was reported.

2.4.7. Mechanical properties

A texture analyser (TA-HD plus, Stable Micro Systems, UK) was used to evaluate the mechanical properties of the developed films. The tests were conducted according to the ASTM standard method number D882. The films (cut into rectangular strips of 50 mm by 5 mm) were tensile operated with an initial grasp separation of 40 mm and a crosshead speed of 60 mm/min . The tensile strength (maximum load (N) divided by the initial cross-sectional area (m^2) of the films), breaking strain (percentage extension of the initial length of the films at the breaking point) and toughness (energy per unit volume to break) were determined as reported by [Santhosh and Sarkar \(2022\)](#).

2.4.8. Water vapour permeability

The water vapour transmission rate (WVTR) of the films was determined using Mocon Permatran-W[®] 3/34 (G) (Ametek Mocon, Minneapolis, US) at $50\text{ }^\circ\text{C}$ and 80% relative humidity in compliance with ASTM F1249. The sample area was 50 cm^2 . Water vapour permeability (WVP) was derived using the equation below:

$$WVP = \frac{WVTR \times h}{\Delta P} \quad (1)$$

Where h is the film thickness and ΔP is the pressure difference across the film.

2.5. Statistical analysis

Experiments were conducted at least in duplicate. Means were obtained and separated using one-way analysis of variance and Duncan Multiple Range Test, respectively in IBM SPSS statistics 28.0

environment. Box plots were generated using R 4.2.2 (R Core Team, 2022). Excel (Microsoft Office 365) was used to generate other plots.

3. Results and discussion

3.1. Rheological properties of the film-forming solution

Control of the rheological properties of film-forming solutions is important in the fabrication of composite films ([Lipatova et al., 2020](#)). Data from rheological measurements give useful information on the nature and contribution of materials in the matrix, the extent of hydrolysis and homogeneity of the solutions, and could have a bearing on the final quality of the prepared films ([Alimi, Workneh, & Oyeyinka, 2017](#); [Liu et al., 2020](#)). The boxplots of shear viscosity and shear modulus (elastic and viscous) of the film-forming solutions are presented in [Fig. 1](#). An increase in the studied rheological properties was observed for the increased chitosan content of the composite blends. Increased shear viscosity and shear modulus with increasing chitosan content could reflect greater interactions between reactive groups of chitosan (NH_2 and OH), starch (OH) and hydrophilic end of glycerol in the solution ([Liu et al., 2012](#)). It could be that the rising chitosan content was making more reactive groups available for the interactions. The same phenomenon may explain the higher viscosity and modulus values of sample 3 despite having the same chitosan content as the control (sample 4). [Huang, Winkler, & Sutmann \(2010\)](#) reported that the viscous flow of a polymeric material was due to the shift of the centre of gravity of the molecular network along the direction of the flow and the slides within the matrix. Increasing the chitosan content could induce greater segmentation within the matrix; hence, more time would be needed to achieve synergies and transfer of the centre of gravity ([Liu et al., 2020](#)). Hence, increased shear viscosity and modulus of the film-forming solution with increasing chitosan content led to reduced mobility of the solution.

3.2. Morphological properties of the films

3.2.1. Surface and cross-sectional structures of the films

Changes in the structure of the films were captured with a scanning electron microscope ([Fig. 2](#)). Generally, films exhibited a smooth and closely packed surface devoid of large pores and cracks. This is an indication of the blending of chitosan and potato starch at the microstructural level. [Liu et al. \(2020\)](#) reported that high MW chitosan gives a closely knitted film structure. Formation of hydrogen bonds from the interaction of the $-\text{OH}$ and $-\text{COH}$ side groups of the starch with the $-\text{NH}_2$ and $-\text{OH}$ groups of chitosan may be responsible for this smooth and closely packed surface ([Liu et al., 2012](#)). Also, the formation of polyanion-polycation complexes from a cross-linking network formed through the covalent and non-covalent bonding of chitosan and starch might play a significant role in the smooth surfaces observed for the composite films. This phenomenon might be responsible for the highly viscous gel formed between chitosan and starch ([Sionkowska, Wisniewski, Skopinska, Kennedy, & Wess, 2004](#)). Pockets of white patches on the surface of composite films have been previously reported to be due to withered starch and chitosan microgel fraction ([Lipatova et al., 2020](#)).

The cross-sectional images of the films also confirmed the homogeneous and compact structure of the films ([Fig. 2b](#)). [Bof, Bordagaray, & Locaso \(2015\)](#) in a previous study reported that high molecular weight chitosan gave compact structure.

3.2.2. Surface roughness of the films

The 3D plots of the surface roughness of the films are presented in [Fig. 3](#). Contrary to the near-smooth surfaces obtained from SEM images, AFM showed some protrusions on the surface of the films which indicated some degree of heterogeneity of their matrices ([Wu, Lei, et al., 2019](#)). [da Muta da Mata Cunha, Lima, Assis, Tiera, and de Oliveira Tiera \(2020\)](#) attributed the protrusion on the surfaces of chitosan-based films

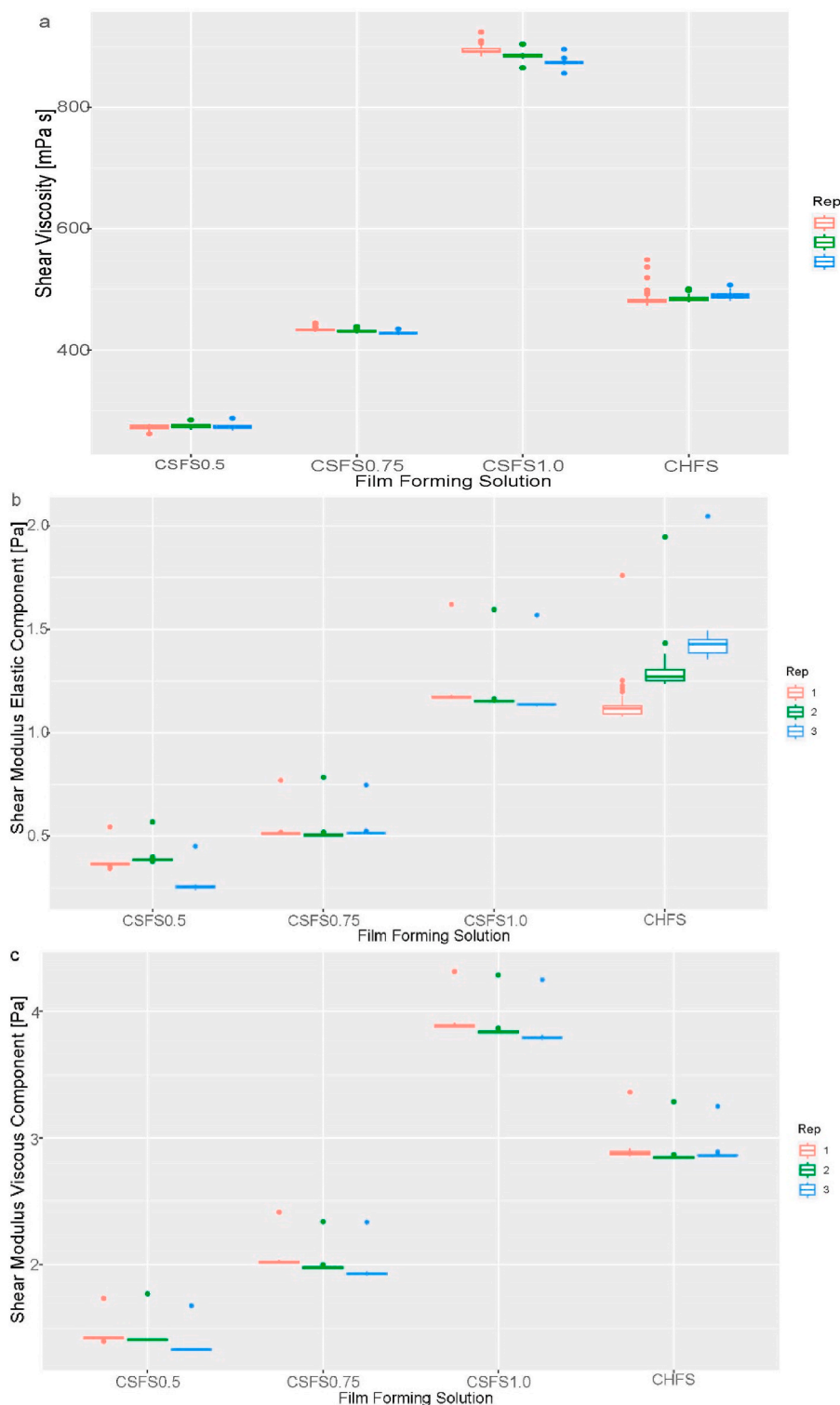


Fig. 1. Box plots of the rheological properties of the film-forming solutions.

(CSFS0.5: FFS containing chitosan of 0.5% in the solution; CSFS0.75: FFS containing chitosan of 0.75% in the solution; CSFS1.0: FFS containing chitosan of 1.0% in the solution; CHFS: FFS containing 1.0% chitosan in the solution, and without potato starch (control).

to the clustering of the hydrophilic component in the films' matrices. The protrusion or mountain-like structure was decreasing with increasing chitosan content. This could be related to increasing interaction within the chain to create hydrophilic-hydrophobic balance thereby promoting intermolecular entanglement and cohesion within the network (Zhong, Zhuang, Gu, & Zhao, 2019). A comparatively higher clustering was observed in the reference film against the

composite film of the same chitosan content. This can be attributed to more availability of unreactive sites. The empirical data of surface roughness (the surface roughness of the composite films decreased with increasing chitosan content (CSF0.5: 19 ± 2 nm; CSF0.75: 8.5 ± 0.5 nm; CSF1.0: 6 ± 2 nm) while pure chitosan film (control) had a higher value (CHF: 17 ± 3 nm) than the composite film of the same chitosan content) correlated well with the 3D visual observation.

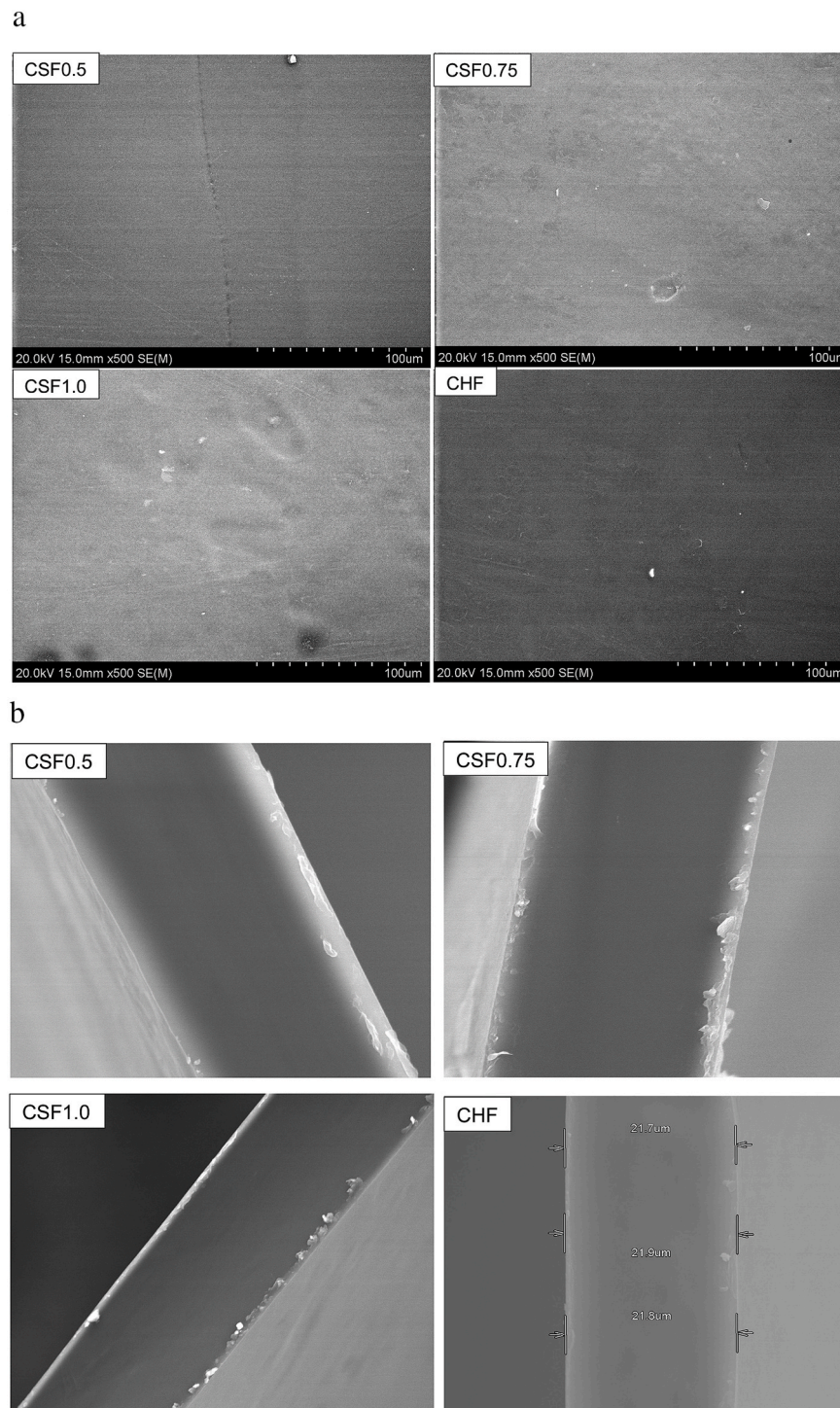


Fig. 2. Scanning electron micrographs of (a) the surfaces and (b) the cross-sections of the films.

CSF0.5: Composite film containing chitosan of 0.5% in the FFS; CSF0.75: Composite film containing chitosan of 0.75% in the FFS; CSF1.0: Composite film containing chitosan of 1.0% in the FFS; CHF: Film containing 1.0% chitosan of the FFS, and without potato starch (control).

3.3. XRD

All films in this study exhibited similar diffraction conformation (Fig. 4). The only discernible peak for the films was a broad peak around 20° (2θ). A minor peak was observed around 9° . A similar diffraction pattern of a broad crystalline peak was obtained for films developed from chitin extracted from crustacean waste (Saravana et al., 2018). The broad peak could be an indication of a well-arranged long-range structure (Qiao, Ma, Wang, & Liu, 2021). Chitosan-based films were reported

by Shariatinia and Fazli (2015) to exhibit two hydrated crystalline phases: Stable T phase at around 9° and 20° and metastable L-2 phase at around 7° and 16° . Chitosan films developed in this study showed only a stable crystalline phase. Zhuang, Zhong, and Zhao (2019) demonstrated that the presence of the stable crystalline phase could be attributed to the formation of hydrogen bonds. The hydrogen bonds held the matrix firmly thereby giving a compact and cohesive structure (Ziani, Oses, Coma, & Maté, 2008). This attribute may be due to the high molecular weight of the chitosan used in this study. da Mata Cunha et al. (2020)

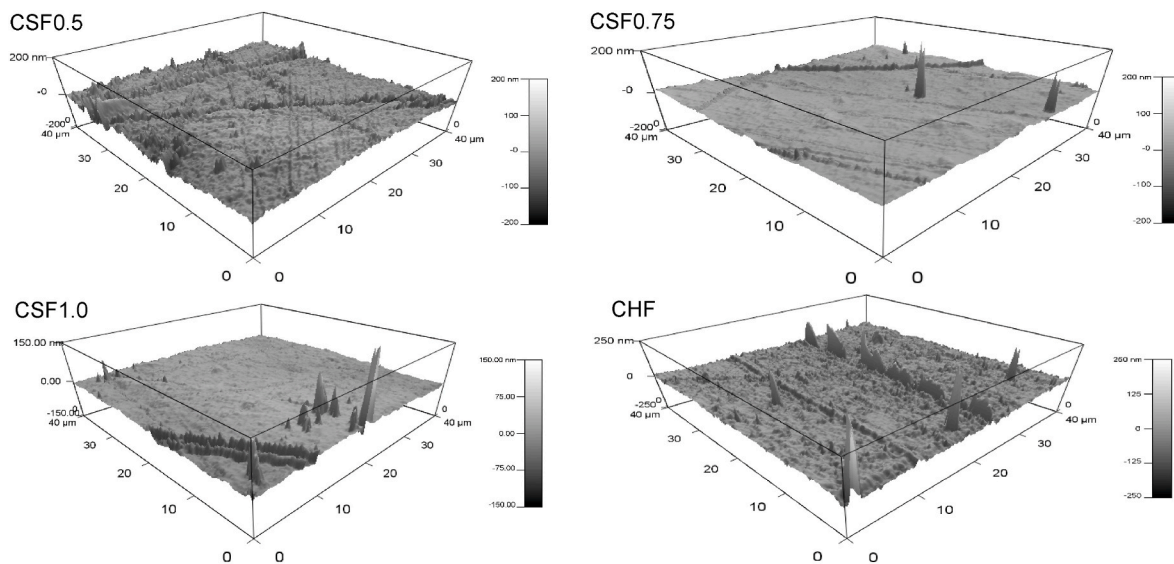


Fig. 3. 3D plots showing the roughness of the surface of the films.

CSF0.5: Composite film containing chitosan of 0.5% in the FFS; CSF0.75: Composite film containing chitosan of 0.75% in the FFS; CSF1.0: Composite film containing chitosan of 1.0% in the FFS; CHF: Film containing 1.0% chitosan of the FFS, and without potato starch (control).

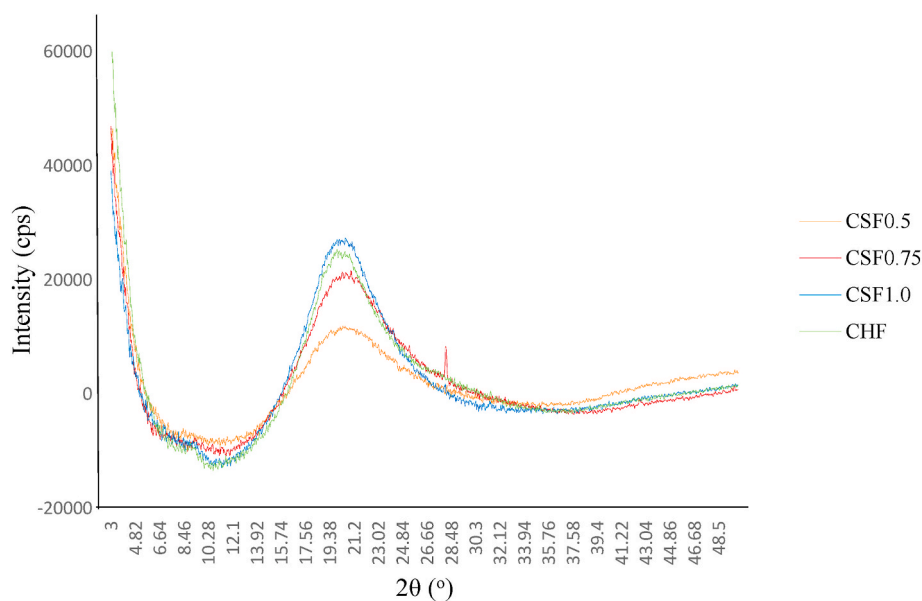


Fig. 4. X-ray diffraction patterns of the films.

CSF0.5: Composite film containing chitosan of 0.5% in the FFS; CSF0.75: Composite film containing chitosan of 0.75% in the FFS; CSF1.0: Composite film containing chitosan of 1.0% in the FFS; CHF: Film containing 1.0% chitosan of the FFS, and without potato starch (control).

also reported a stable T phase crystallinity for high molecular weight chitosan-based films. This stable crystallinity form imparted could be the result of a stronger propensity of high molecular weight chitosan for molecule assembly and self-aggregation (Zhong et al., 2019).

3.4. Optical properties

The optical properties of films are important quality parameters that could have a bearing on their visual appearance as perceived by consumers and offer protection against the loss of light-sensitive constituents of the packaged foods (Alimi et al., 2022; Alimi, Shittu, & Sanni, 2014). Generally, the developed films showed light transmittance in the range of 78.54–87% (Table 1). An initial increase in the chitosan content (from 0.5 to 0.75%) led to a significant ($p < 0.05$) increase in the light

transmittance of the film. A following increase in chitosan content did not lead to a significant light transmission change. The comparatively higher transmittance values (86.5–90.4%) with a similar trend as observed in this study were also reported for chitosan-based films by Lin et al. (2020). Zhao, Teixeira, Gänzle, and Saldaña (2018) linked the higher light transmittance to minimal light scattering due to the near homogeneity of the matrices.

Glossiness measured at 20 and 60° increased with increasing chitosan content. The increase was significant at 20° for every chitosan content increment, while films (composite and control) with the highest chitosan content had significantly higher glossiness than others, similar to a previous report (Othman, Othman, Shapi'i, Ariffin, & Yunus, 2021). It is important to point out that gloss values increased with decreasing surface roughness of the films. That is, a film with a smoother surface

Table 1
Optical, mechanical and moisture barrier properties of the films.

Sample	Light transmittance (%)	Glossiness		Thickness (mm)	Strength (MPa)	Breaking strain (%)	Toughness (MJ/m ³)	WVP (10 ⁻¹³ g/m ² s Pa)
		20 (°)	60 (°)					
CSF0.5	78.537 ^a ±2.469	4.167 ^a ±1.060	22.967 ^a ±4.997	0.031 ^a ±0.005	19.001 ^a ±0.212	60.968 ^a ±0.008	0.093 ^a ±0.004	0.991 ^a ±1.073
CSF0.75	86.183 ^b ± 0.450	8.533 ^b ± 0.351	27.167 ^a ±2.483	0.038 ^b ± 0.009	24.137 ^b ± 0.966	63.644 ^a ±0.495	0.631 ^a ±0.100	2.401 ^{ab} ± 0.180
CSF1.0	86.997 ^b ± 0.518	13.067 ^c ±0.945	65.800 ^b ± 5.897	0.042 ^b ± 0.011	24.700 ^b ± 0.441	71.540 ^b ± 5.320	2.442 ^b ± 1.272	2.649 ^b ± 0.109
CHF	84.167 ^b ± 4.606	14.533 ^c ±0.764	75.267 ^b ± 13.661	0.025 ^a ±0.006	29.302 ^c ±2.412	62.002 ^a ±0.905	0.354 ^a ±0.212	1.950 ^{ab} ± 0.117

Average ± standard deviation. The letter indicates significant differences (post hoc test with $p < 0.05$) between Samples.

CSF0.5: Composite film containing chitosan of 0.5% of the film-forming solution; CSF0.75: Composite film containing chitosan of 0.75% of the film-forming solution; CSF1.0: Composite film containing chitosan of 1.0% of the film-forming solution; CHF: Film containing 1.0% chitosan of the film forming solution and without potato starch (control).

offered a higher gloss value. This observation is consistent with the miscible compatibility of starch and chitosan. The miscibility promoted homogeneity in the matrix thereby limiting the scattering of particles on the surfaces of the films (Zhao et al., 2018).

3.5. FTIR

The development of films in this study occurred through the complex interactions of the high molecular weight chitosan from *A. bisporus*, potato starch and glycerol at a high temperature of 95 °C. The changes induced by the creation of covalent chemical bonds were captured using an FTIR spectroscope. All the developed films in this study displayed a similar spectrum as shown in Fig. 5. The complex vibrational hydrogen bonding of NH₂ from chitosan and OH from starch is responsible for the prominent broadband at 3600 to 3000 cm⁻¹ (Lin et al., 2020). In the case of the film made from chitosan alone, the band can be attributed to the interaction of NH₂ and OH within its system (Zhao et al., 2018). This interaction is the primary mode of interaction of most hydrophilic polymers and is indicative of the formation of intra and intermolecular networks within the film matrix (Bof, Bordagaray, Locaso, & García, 2015). Notably, the film with the highest chitosan content and the control exhibited a wide band in this region. The higher chitosan content of this film made more amino and hydroxyl groups available for reaction and for the formation of hydrogen bonds for inter and intra-molecular cohesion (Zheng, Tang, & Li, 2022).

The observed transmittance band between 3000 and 2700 cm⁻¹ is

typical of the vibrational stretching of the CH bond (Alimi et al., 2022). Similarly, the observed band at 2100 cm⁻¹ region indicated the presence of nitrile (NH) functional groups. An equivalent band was identified for some chitosan films at 2100 nm using near infra-red spectroscopy by Cervera et al. (2004). The stretching vibration of the carbonyl group of chitosan was responsible for the transmittance peaks at 1640 and 1549 cm⁻¹ (Lin et al., 2020). These bands indicated the presence of amide-1 and amide-2 reactive groups, respectively (Zhao et al., 2018). They were reported to be the characteristic peaks, which are the fingerprint regions, of chitin and chitosan (Saravana et al., 2018).

A transmittance peak identified at around 1400 cm⁻¹ is within the band attributed to the aromatic stretching of the carboxyl (COO) group while the peaks identified in the region of 1100-900 cm⁻¹ related to the vibration of C-O, C-O-H and C-O-C in the glycosidic skeleton of the matrices (Alimi & Workneh, 2018; Santhosh & Sarkar, 2022). The prominence of the bands at around 900 cm⁻¹ could also indicate the comparative differences in the crystallinity of the films (Alimi & Workneh, 2018). The presence of peaks in the region of 700 cm⁻¹ was indicative of the presence of phenolic compounds in the matrices (Alimi & Workneh, 2018).

3.6. Thickness

The thickness of the developed films is presented in Table 1. Controlling the thickness of the film is a crucial processing step during the manufacture of the film because it affects the barrier of films to gases

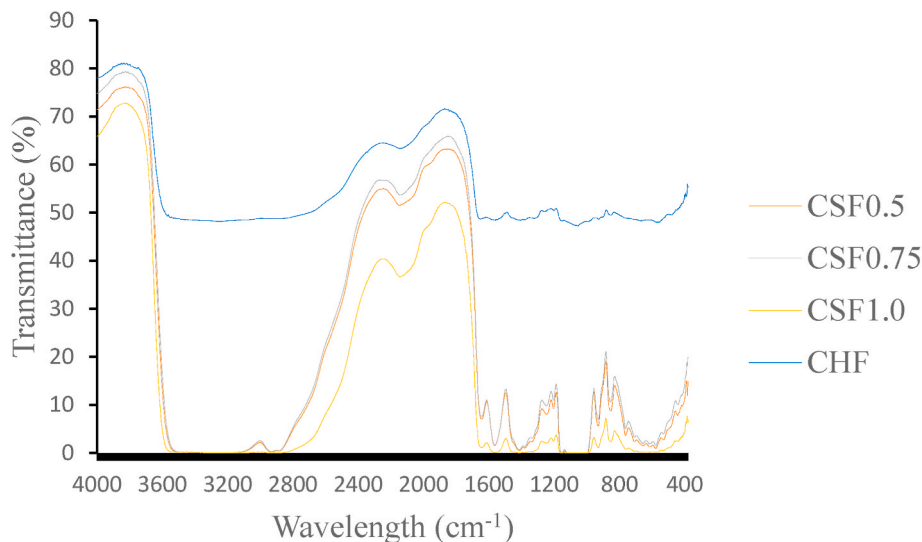


Fig. 5. FTIR spectra of the films.

CSF0.5: Composite film containing chitosan of 0.5% in the FFS; CSF0.75: Composite film containing chitosan of 0.75% in the FFS; CSF1.0: Composite film containing chitosan of 1.0% in the FFS; CHF: Film containing 1.0% chitosan of the FFS, and without potato starch (control).

and water vapour pressure (Alimi et al., 2022). Increasing chitosan content led to an increase in the thickness of the composite film. However, only the first increase of chitosan gave a significant ($p < 0.05$) change in the thickness of the composite film. The increased interaction between the reactive groups of chitosan and starch may have led to increased density of the composite films thereby imparting their thickness (Lin et al., 2020). Sani, Pirsá, and Tađi (2019) observed that the addition of more chitosan increased the solid content within the film and thereby gave a denser structure. This could also explain the generally higher thickness of the composite films over the control.

3.7. Mechanical properties of the films

All the investigated mechanical properties (strength, breaking strain, and toughness) increased with chitosan content (Table 1). Lin et al. (2020) also reported a similar trend in their study on chitosan-based composite films. Zhao et al. (2018) concluded that the formation of more hydrogen bonds, which led to increased inter and intramolecular cohesion, improved the mechanical structure of the films. Wu, Lei, et al. (2019) attributed the improved mechanical properties to intra and inter-molecular crosslinking among the reactive sites of chitosan and starch. These were also the findings from SEM, XRD and FTIR analyses in this study.

3.8. Thermal stability of the films

The TGA and DSC plots showing the thermal stability of the films are presented in Fig. 6 (a and b, respectively). Two degradation steps were discernible in the TG curves of the films. The first one started around 91 °C. The mass loss at this stage was reported to be due to the loss of loose and bound water (da Mata Cunha et al., 2020). The second stage, which showed a major mass loss, started at 233–244 °C. The weight loss at this stage was linked to processes that led to the breakdown of the films. The processes included the loss of mass of water of the saccharide rings, depolymerisation and disintegration of acetylated and deacetylated units in the matrices (Wu, Lei, et al., 2019). About 20% of the weight was lost by the films before the onset of the second stage. Composite films exhibited higher stability than the control at this stage. However, composite films showed more weight loss at the end of the stage. Overall, the control film had more remnants than the composite films.

The endothermic and exothermic peaks observed for the films from the DSC curves corresponded to the onset and peak of the major degradations observed in the TGA curves. The endothermic peaks could relate to the disintegration of the acetyl-glucosamine backbone of the chitosan units in the films (Saravana et al., 2018). Its increase with increasing chitosan content could indicate increased crystallinity and tightly held and orderly structure within the film matrices which

required more breakdown energy (Kaya et al., 2022). The exothermic peak that followed may be attributed to the breakdown of hydrogen bonds and other polymeric networks within the films (Saravana et al., 2018). The XRD report of films in this study had shown an enhanced stability of the crystalline structure of the films with the increase in chitosan content while the SEM report indicated a more compact structure with the chitosan content. The FTIR also showed an interaction in the primary mode of most hydrophilic polymers, which indicated the formation of intra and intermolecular networks within the film matrix. This interaction was spotted in the region known for the vibrational hydrogen bonding.

3.9. Water vapour permeability (WVP)

The packaging material's water vapour permeability (WVP) is a significant factor that directly affects the shelf life of packaged foods (Alimi et al., 2022). The WVP values obtained for the *A. bisporus* chitosan-based films in this study (Table 1) were much lower than values reported for marine-sourced chitosan-based films in some previous studies (a hundredth (Liu et al., 2014) and a thousandth (Bof et al., 2015)). The *A. bisporus*-sourced chitosan presented a more compact structure (as shown in the SEM, XRD and FTIR reports of the films in this study) and hence, higher resistance to vapour movement. This lower WVP is an indication that they would offer higher control over moisture movement. The increased WVP with the increasing chitosan content was previously reported to be due to chitosan's general hydrophilic nature, which promoted the migration of moisture across the films and improved the subsequent interaction with water molecules (Lin et al., 2020). The WVP of pure chitosan film was higher than that of the composite film with the same content of chitosan. A reduction in the availability of hydrophilic groups due to the formation of hydrogen bonds between the reactive groups of potato starch and chitosan, leading to reduced polymeric mass, may have engendered a rigid microstructure that restricted moisture movement (Bof et al., 2015; Liu et al., 2012).

4. Conclusions

The rheological properties of the film-forming solutions in this study were influenced by the chitosan content: shear viscosity and shear modulus (elastic and viscous components) increased with chitosan content. The morphological observations revealed a near-homogenous and compact structure with surface roughness reducing with increasing chitosan content in the film. Greater interactions of reactive groups of the polymers were identified from the FTIR spectra. The increasing content of chitosan resulted in the development of stronger and more intense hydrogen bonds which led to improved inter and intra-molecular cohesion within the film matrix. This explained the enhanced

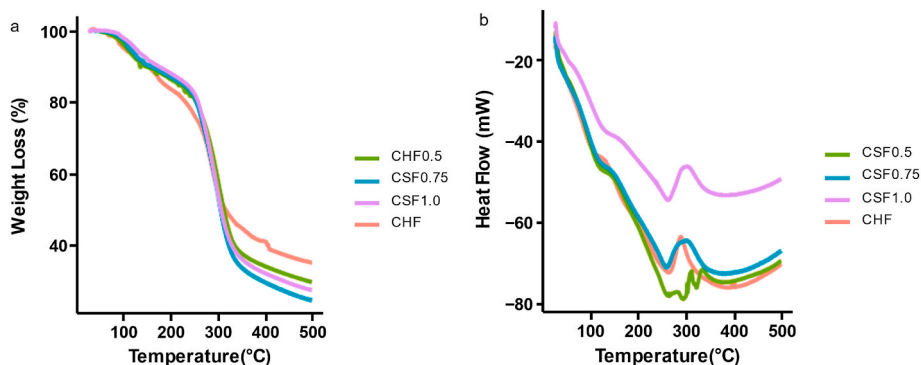


Fig. 6. Thermal properties of the films (a: TGA; b: DSC).

CSF0.5: Composite film containing chitosan of 0.5% in the FFS; CSF0.75: Composite film containing chitosan of 0.75% in the FFS; CSF1.0: Composite film containing chitosan of 1.0% in the FFS; CHF: Film containing 1.0% chitosan of the FFS, and without potato starch (control).

mechanical and water barrier properties of the films. *A. bisporus* chitosan-based films generally showed excellent optical characteristics. This is of commercial benefit as aesthetically pleasing packaging can help buyers accept some products more readily.

Therefore, this work has laid a foundation for the prospective use of chitosan derived from button mushrooms in the development of films for food packaging.

Funding

This work was supported by Marie Slodowska-Curie and Enterprise Ireland through CAREER-FIT PLUS Fellowship (MF 2021 0199) granted to Dr Buliyaminu Adegbemiro Alimi.

CRediT authorship contribution statement

B. A. Alimi: Conceptualisation, investigation, data curation, writing-original draft. M. Hoque: PhD student, conducted some components of the laboratory investigation. S. Pathania: A collaborator on the project, some laboratory analyses were conducted in her laboratories, reviewed, and edited the draft manuscript. Jude Wilson: The industry mentor to B. A. Alimi, reviewed the draft manuscript. Brendan Duffy: A collaborator on the project, some characterisation tests were conducted in his laboratory and reviewed the manuscript. J. M. Frias: Academic mentor to B. A. Alimi, data analysis, reviewed and edited the draft manuscript.

Declaration of generative AI and AI-assisted technologies in the writing process

During the preparation of this work, the author(s) used 'GRAMMARLY' in order to improve the READABILITY of the manuscript. After using this tool/service, the author(s) reviewed and edited the content as needed and take(s) full responsibility for the content of the publication.

Declaration of competing interest

Authors declare no conflict of interest.

Data availability

Data will be made available on request.

Acknowledgements

The authors acknowledge the kind supply of potato starch by Finnegan's Farm, Navan, Co. Meath, Ireland. The efforts of the following individuals toward the success of this study are greatly appreciated: Elena Irina Pascu (CREST), Joseph Mohan (CREST), Wasim Bashir (CREST), Fredrick Odunjo (CREST), Aaron Byrne (CREST), Luke O. Neill (FOCAS) and Denise Denning (FOCAS).

References

- Alimi, B. A., Shittu, T. A., & Sanni, L. O. (2014). Effect of hydrocolloids and egg content on sensory quality of coated fried yam chips. *Journal of Culinary Science & Technology*, *12*(2), 168–180.
- Alimi, B. A., & Workneh, T. S. (2018). Structural and physicochemical properties of heat moisture treated and citric acid modified acha and iburu starches. *Food Hydrocolloids*, *81*, 449–455.
- Alimi, B. A., Workneh, T. S., & Femi, F. A. (2021). Fabrication and characterization of edible films from acha (*Digitalia exilis*) and iburu (*Digitalia iburua*) starches. *CyTA—Journal of Food*, *19*(1), 493–500.
- Alimi, B. A., Workneh, T. S., & Oyeyinka, S. A. (2017). Structural, rheological and in-vitro digestibility properties of composite corn-banana starch custard paste. *LWT—Food Science and Technology*, *79*, 84–91.
- Alimi, B. A., Workneh, T. S., & Zubair, B. A. (2022). Microstructural and physicochemical properties of biodegradable films developed from false banana (*Ensete ventricosum*) starch. *Heliyon*, *8*(3), Article e09148.
- Bof, M. J., Bordagaray, V. C., Locaso, D. E., & García, M. A. (2015). Chitosan molecular weight effect on starch-composite film properties. *Food Hydrocolloids*, *51*, 281–294.
- Bonilla, J., Atarés, L., Vargas, M., & Chiralt, A. (2013). Properties of wheat starch film-forming dispersions and films as affected by chitosan addition. *Journal of Food Engineering*, *114*(3), 303–312.
- van den Broek, L. A., Knoop, R. J., Kappen, F. H., & Boeriu, C. G. (2015). Chitosan films and blends for packaging material. *Carbohydrate Polymers*, *116*, 237–242.
- Cervera, M. F., Karjalainen, M., Airaksinen, S., Rantanen, J., Krogars, K., Heinämäki, J., et al. (2004). Physical stability and moisture sorption of aqueous chitosan-amylose starch films plasticized with polyols. *European Journal of Pharmaceutics and Biopharmaceutics*, *58*(1), 69–76.
- Claro, P. I. C., Neto, A. R. S., Bibbo, A. C. C., Mattoso, L. H. C., Bastos, M. S. R., & Marconcini, J. M. (2016). Biodegradable blends with potential use in packaging: A comparison of PLA/chitosan and PLA/cellulose acetate films. *Journal of Polymers and the Environment*, *24*, 363–371.
- Ghormade, V., Pathan, E. K., & Deshpande, M. V. (2017). Can fungi compete with marine sources for chitosan production? *International Journal of Biological Macromolecules*, *104*, 1415–1421.
- Grimm, D., & Wösten, H. A. (2018). Mushroom cultivation in the circular economy. *Applied Microbiology and Biotechnology*, *102*, 7795–7803.
- Hassainia, A., Satha, H., & Boufi, S. (2018). Chitin from *Agaricus bisporus*: Extraction and characterization. *International Journal of Biological Macromolecules*, *117*, 1334–1342.
- Huang, C. C., Winkler, R. G., Sutmann, G., & Gompper, G. (2010). Semidilute polymer solutions at equilibrium and under shear flow. *Macromolecules*, *43*(23), 10107–10116.
- Kannan, M., Nesakumari, M., Rajarathinam, K., & Singh, A. J. A. R. (2010). Production and characterization of mushroom chitosan under solid-state fermentation conditions. *Advances in Biological Research*, *4*(1), 10–13.
- Kaya, E., Kahyaoglu, L. N., & Sumnu, G. (2022). Development of curcumin incorporated composite films based on chitin and glucan complexes extracted from *Agaricus bisporus* for active packaging of chicken breast meat. *International Journal of Biological Macromolecules*, *221*, 536–546.
- Lin, D., Zheng, Y., Huang, Y., Ni, L., Zhao, J., Huang, C., et al. (2020). Investigation of the structural, physical properties, antioxidant, and antimicrobial activity of chitosan-nano-silicon aerogel composite edible films incorporated with okara powder. *Carbohydrate Polymers*, *250*, Article 116842.
- Lipatova, I. M., Losev, N. V., Makarova, L. I., Rodicheva, J. A., & Burmistrov, V. A. (2020). Effect of composition and mechanoactivation on the properties of films based on starch and chitosans with high and low deacetylation. *Carbohydrate Polymers*, *239*, Article 116245.
- Liu, Z., Ge, X., Lu, Y., Dong, S., Zhao, Y., & Zeng, M. (2012). Effects of chitosan molecular weight and degree of deacetylation on the properties of gelatine-based films. *Food Hydrocolloids*, *26*(1), 311–317.
- Liu, Y., Yuan, Y., Duan, S., Li, C., Hu, B., Liu, A., et al. (2020). Preparation and characterization of chitosan films with three kinds of molecular weight for food packaging. *International Journal of Biological Macromolecules*, *155*, 249–259.
- Liu, M., Zhou, Y., Zhang, Y., Yu, C., & Cao, S. (2014). Physicochemical, mechanical and thermal properties of chitosan films with and without sorbitol. *International Journal of Biological Macromolecules*, *70*, 340–346.
- Madeleine-Perdrillat, C., Karbowiak, T., Raya, J., Gougeon, R., Bodart, P. R., & Debeaufort, F. (2015). Water-induced local ordering of chitosan polymer chains in thin layer films. *Carbohydrate Polymers*, *118*, 107–114.
- Ma, X., Qiao, C., Wang, X., Yao, J., & Xu, J. (2019). Structural characterization and properties of polyols plasticized chitosan films. *International Journal of Biological Macromolecules*, *135*, 240–245.
- Marçal, S., Sousa, A. S., Taofiq, O., Antunes, F., Morais, A. M., Freitas, A. C., et al. (2021). Impact of postharvest preservation methods on nutritional value and bioactive properties of mushrooms. *Trends in Food Science and Technology*, *110*, 418–431.
- Martinez-Medina, G. A., Chávez-González, M. L., Verma, D. K., Prado-Barragán, L. A., Martínez-Hernández, J. L., Flores-Gallegos, A. C., et al. (2021). Bio-funcional components in mushrooms, a health opportunity: Ergothioneine and huitlacoche as recent trends. *Journal of Functional Foods*, *77*, Article 104326.
- da Mata Cunha, O., Lima, A. M. F., Assis, O. B. G., Tiera, M. J., & de Oliveira Tiera, V. A. (2020). Amphiphilic diethylaminoethyl chitosan of high molecular weight as an edible film. *International Journal of Biological Macromolecules*, *164*, 3411–3420.
- Oladzadabbasabadi, N., Nafchi, A. M., Ariffin, F., Wijekoon, M. J. O., Al-Hassan, A. A., Dheyab, M. A., et al. (2022). Recent advances in extraction, modification, and application of chitosan in packaging industry. *Carbohydrate Polymers*, *277*, Article 118876.
- Ospina Álvarez, S. P., Ramírez Cadavid, D. A., Escobar Sierra, D. M., Ossa Orozco, C. P., Rojas Vahos, D. F., Zapata Ocampo, P., et al. (2014). Comparison of extraction methods of chitin from *Ganoderma lucidum* mushroom obtained in submerged culture. *BioMed Research International*, *1–7*, 169071.
- Othman, S. H., Othman, N. F. L., Shapi'i, R. A., Ariffin, S. H., & Yunus, K. F. M. (2021). Corn starch/chitosan nanoparticles/thymol bio-nanocomposite films for potential food packaging applications. *Polymers*, *13*(3), 390.
- Prateepchanachai, S., Thakiew, W., Devahastin, S., & Soponronnarit, S. (2017). Mechanical properties improvement of chitosan films via the use of plasticizer, charge modifying agent and film solution homogenization. *Carbohydrate Polymers*, *174*, 253–261.
- Qiao, C., Ma, X., Wang, X., & Liu, L. (2021). Structure and properties of chitosan films: Effect of the type of solvent acid. *LWT—Food Science and Technology*, *135*, Article 109984.
- Rathore, H., Prasad, S., & Sharma, S. (2017). Mushroom nutraceuticals for improved nutrition and better human health: A review. *PharmaNutrition*, *5*(2), 35–46.

- Ren, L., Yan, X., Zhou, J., Tong, J., & Su, X. (2017). Influence of chitosan concentration on mechanical and barrier properties of corn starch/chitosan films. *International Journal of Biological Macromolecules*, *105*, 1636–1643.
- Riaz Rajoka, M. S., Zhao, L., Mehwish, H. M., Wu, Y., & Mahmood, S. (2019). Chitosan and its derivatives: Synthesis, biotechnological applications, and future challenges. *Applied Microbiology and Biotechnology*, *103*, 1557–1571.
- Rodríguez-Núñez, J. R., Madera-Santana, T. J., Sánchez-Machado, D. I., López-Cervantes, J., & Soto Valdez, H. (2014). Chitosan/hydrophilic plasticizer-based films: Preparation, physicochemical and antimicrobial properties. *Journal of Polymers and the Environment*, *22*, 41–51.
- Sani, I. K., Pirs, S., & Tağı, Ş. (2019). Preparation of chitosan/zinc oxide/Melissa officinalis essential oil nano-composite film and evaluation of physical, mechanical and antimicrobial properties by response surface method. *Polymer Testing*, *79*, Article 106004.
- Santhosh, R., & Sarkar, P. (2022). Jackfruit seed starch/tamarind kernel xyloglucan/zinc oxide nanoparticles-based composite films: Preparation, characterization, and application on tomato (*Solanum lycopersicum*) fruits. *Food Hydrocolloids*, *133*, Article 107917.
- Saravana, P. S., Ho, T. C., Chae, S. J., Cho, Y. J., Park, J. S., Lee, H. J., et al. (2018). Deep eutectic solvent-based extraction and fabrication of chitin films from crustacean waste. *Carbohydrate Polymers*, *195*, 622–630.
- Shariatnia, Z., & Fazli, M. (2015). Mechanical properties and antibacterial activities of novel nanobiocomposite films of chitosan and starch. *Food Hydrocolloids*, *46*, 112–124.
- Sionkowska, A., Wisniewski, M., Skopinska, J., Kennedy, C. J., & Wess, T. J. (2004). Molecular interactions in collagen and chitosan blends. *Biomaterials*, *25*(5), 795–801.
- Wu, H., Lei, Y., Lu, J., Zhu, R., Xiao, D., Jiao, C., et al. (2019). Effect of citric acid induced crosslinking on the structure and properties of potato starch/chitosan composite films. *Food Hydrocolloids*, *97*, Article 105208.
- Wu, J., Niu, Y., Jiao, Y., & Chen, Q. (2019). Fungal chitosan from *Agaricus bisporus* (Lange) Sing. Chaidam increased the stability and antioxidant activity of liposomes modified with biosurfactants and loading betulinic acid. *International Journal of Biological Macromolecules*, *123*, 291–299.
- Zhao, Y., Teixeira, J. S., Gänzle, M. M., & Saldaña, M. D. (2018). Development of antimicrobial films based on cassava starch, chitosan and gallic acid using subcritical water technology. *The Journal of Supercritical Fluids*, *137*, 101–110.
- Zheng, T., Tang, P., & Li, G. (2022). Effects of chitosan molecular weight and deacetylation degree on the properties of collagen-chitosan composite films for food packaging. *Journal of Applied Polymer Science*, *139*(41), Article e52995.
- Zhong, Y., Zhuang, C., Gu, W., & Zhao, Y. (2019). Effect of molecular weight on the properties of chitosan films prepared using electrostatic spraying technique. *Carbohydrate Polymers*, *212*, 197–205.
- Zhuang, C., Zhong, Y., & Zhao, Y. (2019). Effect of deacetylation degree on properties of Chitosan films using electrostatic spraying technique. *Food Control*, *97*, 25–31.
- Ziani, K., Oses, J., Coma, V., & Maté, J. I. (2008). Effect of the presence of glycerol and Tween 20 on the chemical and physical properties of films based on chitosan with different degree of deacetylation. *LWT—Food Science and Technology*, *41*(10), 2159–2165.